Umm Al-Qura Univ. J. Sci. Med. Eng. Vol 16,, No.2, pp.17 -31 (2004) 24-11-011 © The University Press

Microwave Mosfet Magnetic Sensor Performance

Mohammed Jameel Alawi

محمد جميل علوي

Member IEEE
Assistant Professor, Electrical Engineering. Dept،.
Umm Al-Qura University, Makkah, Saudi Arabia

أداء المجس الإلكتروني المغناطيسي الذي يعمل بالأمواج الدقيقة

يقدم هذا البحث نموذجاً لكاشف من أجل تحسين جس المجال المغناطيسي الخارجي بإستخدام تقنية الناقل الإلكتروني شبه الموصل المعدني الأكسيدي العامل بالمجال التأثيري في إتجاهين متعامدين إبتداءاً مـن التردد الصفري وحتى ترددات عالية (جيجا هيرتز). و قد تم تطوير نمـوذج التحليـل الرياضـي النظـري وأُستنتجت حساسية النبيطة الإلكترونية و التي تبين مقدار التحسن الكبير و التركيز العالي.

Abstract

This work presents a detector, using MOS technology, for sensing external magnetic fields in two perpendicular directions from dc up to GHz frequencies. Theoretical analysis is developed and the device sensitivity is concluded which shows great improvement as well as higher resolution.

Key words: magnetic field sensors, linear sensor array matrix, splitdrain MOSFET's, magento diodes, magneto transistors,charge coupled devices.

INTRODUCTION

Using MOSFETs as a sensor in magnetic field detection area plays a great role in both Magnetic Field Sensor (MFS) applications such as Charge Coupled Devices (CCD) (Johannes *et al*. 1999; Nixon *et al*. 1997) and Biomedical Diagnosis Systems like Magnetic Resonance Imaging (MRI) and MRI Spectroscopy. A variety of semiconductor devices sensitive to magnetic field have been investigated, including Hall devices, Magneto-diodes, Split-drain MOSFET's, and Magneto-Transistor (MT) (Ristic *et al*. 1989). In the last decade, many authors introduced models to study the effect of magnetic fields on the electrical performance of active devices (Nixon *et al*.1997; Wiliam *et al*. 1993; Ristic *et al*. 1989). These models took into consideration the effect of magnetic field on MESFET (Alsunaidi *et al*. 1996) which, in most cases, was obtained by full coupling of the device transport equation with Maxwell's equations (El-Ghazaly 1997). However, this coupling requires some limitations on operating frequency, device dimensions, and the required high CPU time. In the meantime, there is still a need for magnetic field detectors that operate

over a wide frequency and can be implemented using the well-established manufacturing technology.

The aim of this work is to investigate a detector, which is able to detect the effect of external magnetic field from dc to GHz frequencies by using devices based on MOS technology.

The effect of an external applied magnetic field on the device characteristic, a term which is usually known as device sensitivity, is investigated. At the end of this work we propose the solution of these problems by introducing a construction of x-z directions magnetic field detector based on MOS technology as well as a new system of detection called a linear sensor array matrix (SAM).

DEVICE CONSTRUCTION AND ANALYSIS

Fig.1 shows a top view and cross section of the proposed magnetic sensor. It is constructed of a square-looped source MOSFET surrounded by four lateral MOSFETs whose sources act as current collectors. Two of them (T_1, T_2) are axially located along the x-direction, while the other two (T_3, T_4) are located along the z-direction. The first two collectors (T_1, T_2) are responsible for detecting the z-oriented magnetic fields, while the other two (T_3, T_4) are responsible for detecting the x-field component. If the magnetic field acting in the x-z plane is to be detected, the two pairs of lateral collectors cooperatively function to measure the field intensity and indicate its direction of operation. The square-looped source structure provides a trapezoidal-formed channel, which enhances carrier heating even at small biasing voltages without the need for scaling down the device geometry (Ramadan *et al.* 1999). In the absence of the magnetic field (B = 0), the carrier substrate current penetrates into the bulk and the four lateral collectors accumulate equal currents, where a portion of this current (depending on the substrate bias) goes to the substrate terminal Sb. In the presence of the magnetic field excursion caused by the presence of microwave signal, the symmetry of the substrate current flux is upset in such a manner that one or two collectors (depending on the orientation of B) accumulate more currents than the others. This current difference $\pm\delta I$ -though very small- is converted into a proportional voltage $\pm\delta V$ employing the lateral MOSFETs (T_1, T_2) and (T_3, T_4) as shown in Fig.1.

The operation of the prevoiusly proposed magnetic sensor is based on direct propagation of electrons from the central source to the surrounding collectors. This process is limited only by the propagation delay .

If we process the sensor to operate in the exponential region (low power), then MOSFET current can grow up from 10 pA to 0.1 mA abruptly with a very short delay

(about 10 ps.) (Ramadan *et al*. 1996), which allows the sensor to respond to microwave signals .

From the device construction, the device can detect any field in the x-z plane only and will not respond due to the magnetic field in y-direction. Therefore we can place By = 0 in the equations that determine the current densities J_{nx}, J_{ny} in both the x- and the y- directions (Johannes *et al*. 1999),

$$J_{nx} = -\mu(r+G)J_{ny}\,B_z \quad (1)$$

$$J_{nz} = \mu(r+G)J_{ny}\,B_x \quad (2)$$

$$\delta J_{ny} = \mu(r+G)J_{nx}\,B_z \quad (3)$$

Where: μ is the electron mobility, and r is the scattering factor.

Equation (1) describes the deflection of y-component in the x-direction under the effect of B_z. Also eq. (2) describes the deflection of y-component in z-direction under the effect of B_x. The total current density in x-direction is the sum of all of the current densities changing in the x-direction. Therefor,

$$J_{nx}^{B} = J_{nx}^{0} + \delta J_{nx}^{0} + \delta J_{ny}^{0} \quad (4)$$

Where δJ_{nx}^{0} is given by eqn. (1), δJ_{ny}^{0} is given by eqn. (3), J_{nx}^{0} is the current density at B = 0 and J_{nx}^{B} is the total electron current density in x-direction including the external magnetic field effect .

Similarly the total current density in z-direction is

$$J_{nz}^{B} = J_{nz}^{0} + \delta J_{nz}^{0} + \delta J_{ny}^{0} \quad (5)$$

The sensitivity of the proposed device can be obtained by calculating the sensitivity of T_1 for x-direction as an example. Equation (3) can be rewritten as

$$\delta J_{ny}^{0} = G_x \mu_H\, J_{nx}\, B_z \quad (6)$$

Since the y-component J_{ny} (collected by the substrate terminal) of the current density is in the negative y-direction as shown in Fig.2. Using eq. (1) one can write

$$\delta J_{nx}^{0} = G_y \mu_H\, J_{ny}\, B_z \quad (7)$$

where $Gx = L_x/W_y$, similarly G_y defined as shown in Fig.2 and is given by

$$G_y = L_y/W_x \quad (8)$$

Finally, the total current in the x-direction can be expressed as

$$I_{dx} = I_{d0} + \delta_x I_{s0} + \delta_y I_{d0} \quad (9)$$

where

$$I_{d0} = J_{nx} W_y W_z \tag{10}$$

$$I_{s0} = J_{ny} W_z W_x \tag{11}$$

By substitution eqn. (7) into eqn. (11) one gets:

$$\delta_x I_{s0} = \mu_H B G_y I_{s0} \tag{12}$$

Similarly by substituting eq. (6) for eq. (12) and as shown in Fig.2 one gets:

$$\delta_y I_{d0} = \mu_H B G_x I_{d0} \tag{13}$$

The total change becomes:

$$\Delta I_{dx} = \delta_x I_{s0} + \delta_y I_{d0} \tag{14}$$

By substituting eq. (12) and eq. (13) for eq. (14), one gets :

$$\Delta I_{dx} = \mu_H B \left(I_{s0} \frac{L_y}{W_x} + I_{d0} \frac{L_x}{W_y} \right) \tag{15}$$

The relative sensitivity defined in (Ristic *et al*. 1989) can be set in the form

$$S_r = \mu_H \left(\frac{I_{s0}}{I_{d0}} \frac{L_y}{W_x} + \frac{L_x}{W_y} \right) \tag{16}$$

Adjusting the geometrical parameters and the biasing conditions, we can obtain

$$J_{ny} = K_p J_{nx} \tag{17}$$

where K_p is a proportionality constant depending on the biasing conditions.

By substituting eq. (17) into eq. (16) to find the ratio of I_{s0}/I_{d0} ,

$$\frac{I_{s0}}{I_{d0}} = \frac{J_{ny} W_x}{J_{nx} W_y} = \frac{K_p J_{nx} W_x}{J_{nx} W_y} = K_p \frac{W_x}{W_y} \tag{18}$$

Similarly, substituting eq. (18) for eq. (16) one gets the relative sensitivity S_r as:

$$S_r = \frac{\mu_H}{W_y} \left(K_p L_y + L_x \right) \tag{19}$$

The relative sensitivity of the normal MOSFET device S_r^{MOS} (Ristic *et al*. 1989) is given by

$$S_r^{MOS} = \mu_H \frac{L_x}{W_y} \tag{20}$$

Then the relative sensitivity of our proposed device interms of S_r^{MOS} is given by

$$S_r^{Dev} = \frac{\mu_H}{W_y} K_p L_y + S_r^{MOS} \quad (21)$$

To obtain higher sensitivity we may assume $L_y = L_x$ then،

$$S_r^{Dev} = S_r^{MOS}\left(K_p + 1\right) \quad (22)$$

From the above discussion we can conclude the following advantages:
(i) this device structure can detect any field in x-z plane, (ii) higher sensitivity can be obtained as compared with the normal MOSFET, and (iii) higher resolution can be achieved.

PROPOSED SYSTEM FOR DETECTION

In this section, we will build the system for detection step by step. The first step is to find the results obtained from analyzing the equivalent circuit using SPICE circuit simulation. The second step is an example of vector field in x-z plane with an angle of deflection with x-axis. The third step is the combination of Magnetic Sensor Pixel (MSP) elements to build the overall system of detection as well as its specifications and requirements.

Equivalent Circuit with Magnetic Coupling

The first step is to modify the normal equivalent circuit by adding the Magnetic Coupling Effect (MCE), which is a new idea to use circuit for SPICE circuit simulation as shown in Fig.3 so as to simulate all pairs of the device (two for x-direction and two for z-direction). Fig. 3 depicts the adjoined Voltage-Controlled Current Source (VCCS) δI_1 and δI_2 to the two current sources I_1 and I_2, respectively (parallel connection to add or subtract the effects of δI_1 or δI_2). The controlling voltage of the two VCCS is the voltage source V_i connected with the transconductances g_1 and g_2. Both g_1 and g_2 have opposite polarity because the current increases in one branch but decreases in the other. The output will be aquired from the difference between V_{C1} and V_{C2} , pictured in Fig.4. The voltage V_x presents the output voltage produced by the x-direction field, while, V_z is produced by the field in z-direction. The privilege of using V_x and V_z is to determine the orientation of the applied field by measuring the angle between V_x and V_z as will be explained later in the next sections.

To study the effect of external magnetic field on the equivalent circuit, we must find δI. From the previous section, δI can be set in the following form (Ristic *et al*. 1989):

$$\delta I = G\mu_H B I_B \quad (23)$$

Where I_B is the substrate current and G is the geometrical correction factor .

SPICE SIMULATION RESULTS

Applying an External dc Field

Simulation is achieved for the equivalent circuit shown in Fig.3. First, the behaviour of δI as V_i varies as shown in Fig.5.

As observed from Fig.5, the relation between *B* and δI is linear which was previously proved . Through adding another horizontal axis for V_i , it is clear that every one volt is equal to 10 mT. The output voltages V_{C1} and V_{C2} as function of *B* are shown in Fig.6. It is clear that the output is increasing in one branch while it is decreasing in the other. To obtain double the output difference ($2\delta V$), the difference between V_{C1} and V_{C2} ($V_{C1} - V_{C2}$) is taken.

Applying an external ac Field

An ac field is applied with a peak voltage with 2V and 100 GHz (equivalent to 20 mT). The simulation results of this case are shown in Fig.8. The output voltages V_{C1} and V_{C2} are shown together in Fig.8a where the phase difference between them is equal to 180°. Double the output is shown in Fig.8b, which is one of the benefits of the proposed MSP. The relationship between the magnitude variation of the applied field and the output difference (V_{C1}-V_{C2}) is shown in Fig.9. The linear relation is verified by changing the magnitude of the field from 10 mT to 40 mT. Fig. 10 plots (V_{C1}-V_{C2}) for different field values.

Applying ac Field with Deflection Angle

The above results were based on the assumption that the applied field is perpendicular to x-axis in x-z plane (+z or -z direction). In this section, we assume that we have a field vector which makes an angle 30° (as an example) with x-axis and is in the x-z plane, and has magnitude of 20 mT (equal to 2V applied in the SPICE simulation) with a frequency of 100 GHz. Then this field will be analyzed in two components one in x-direction and the other in z-direction by using the proposed 30°deflection angle.

Using the equivalent circuit shown in Fig.3, the simulation results for the difference (V_{C1}-V_{C2}) for both field components are shown in Fig.11. If we plot V_z against V_x by using V_x as the horizontal axis and V_z as the vertical axis, we can see the deflection of the vector field with respect to x-axis as depicted in Fig.12. Therefore orientation of any vector field in x-z plane can be determined by measuring V_x and V_z from our MSP.

THE PROPOSED SYSTEM AND ITS REQUIREMENTS

The wave propagation analysis can be used inside the MSP to take into account the effect of the microwave signal on the internal fields and current densities if the device (MSP) and circuit having critical dimensions can be comparable to the wavelength (Alsunaidi *et al*. 1996). Since in our case the MSP dimensions (in the range of μm) are less than the wave length (in the range of mm), there is no need to the wave propagation analysis inside the MSP like (El-Ghazaly 1997). We assume that the microwave signal treats the MSP as a point because it does not propagate through it. This assumption leads to the lumped-element approach (Andreas *et al*. 1999).

A linear sensor array matrix (SAM) (Nixon *et al*.1997) is designed as shown in Fig.13. This array contains several identical MSP arranged in rows and columns. So, any MSP can be selected to get the output (V_x and V_z) by using the appropriate MSP address. The requirement is that the dimensions of this SAM must be greater than the wave length in order to allow the wave to propagate through the SAM. The deflection angle of the applying field is determined by measuring the outputs (V_x and V_z) of each MSP. Also the time of scanning is greater than the wave period. From these outputs, the orientation of the applied field can be determined as discussed in the previous section and Fig.12. Finally, the proposed system for detection is shown in Fig.14.

CONCLUSIONS

This work presents a sensor, that uses the MOS technology. The proposed sensor is able to detect the external magnetic fields in two perpendicular directions from dc up to GHz frequencies. Theoretical analysis is developed, and the device exhibits remarkable improvement in both its sensitivity and resolution. SPICE simulation results show excellent agreement with the theoretical expectations. Finally, a linear sensor array matrix is proposed for precious detection of magnetic fields.

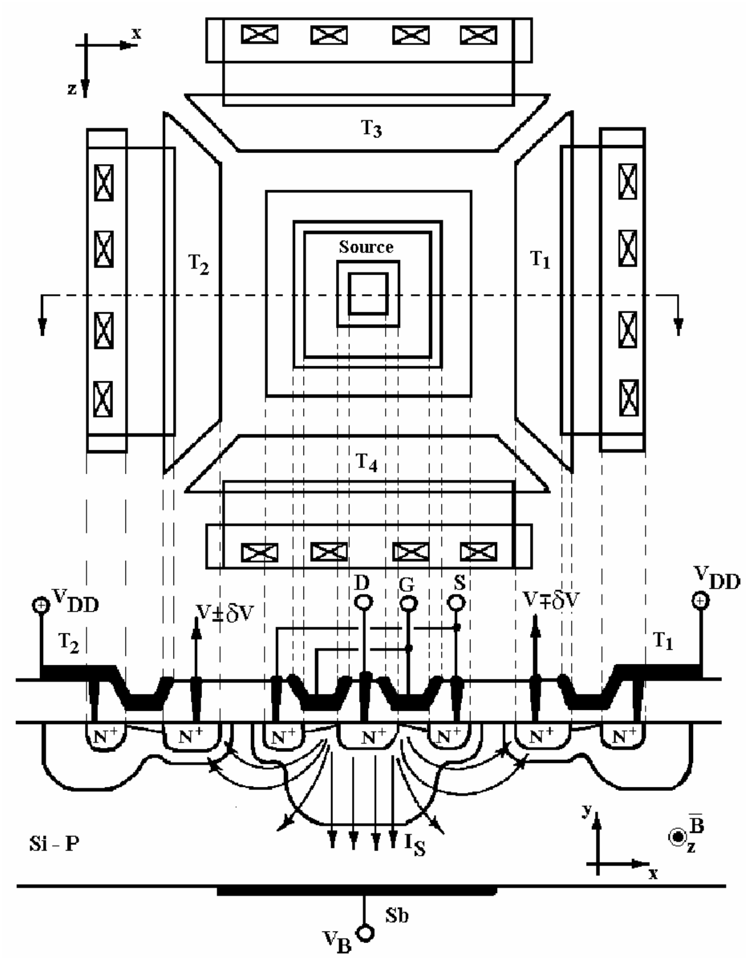


Fig.1 A top view and cross section in the sensor.

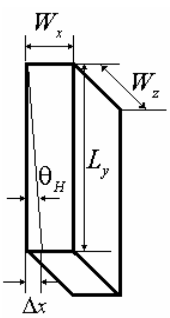


Fig.2 Vertical current (Substrate) is in the negative y-direction.

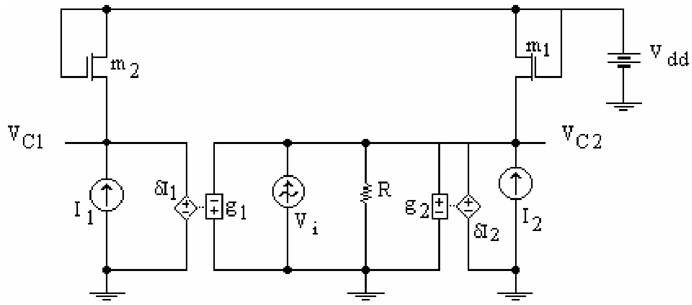


Fig.3 The equivalent circuit with magnetic coupling used in SPICE.

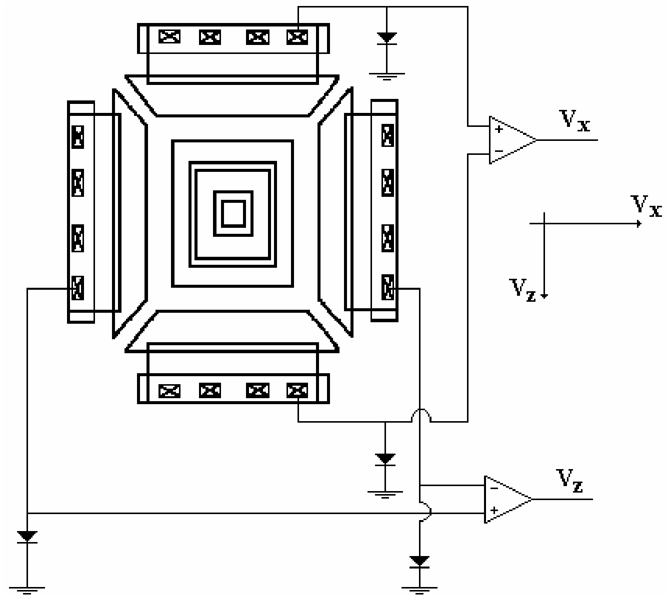


Fig.4 The output voltage from each pair of the Magnetic Sensor Pixel (MSP).

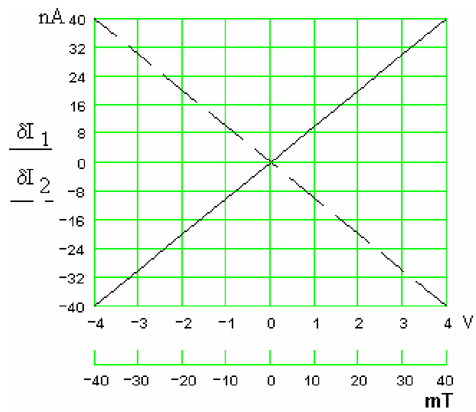


Fig.5. δI against B

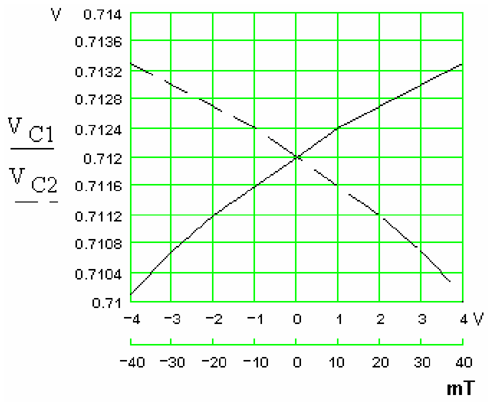


Fig.6 Output $V_1$and V_2 versus B.

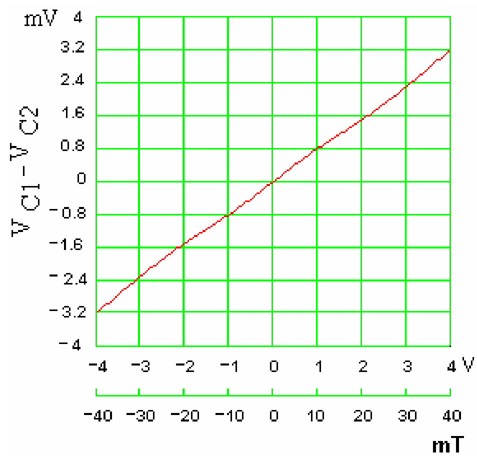
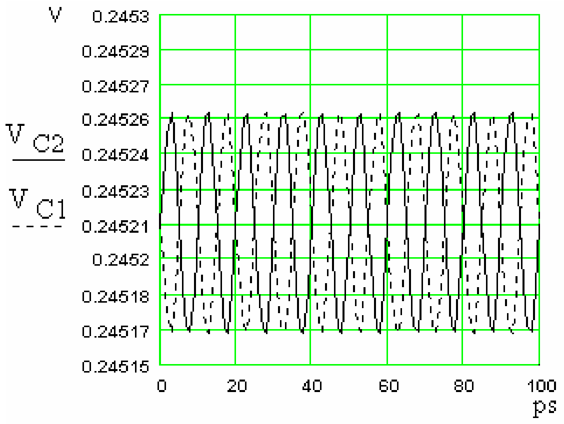
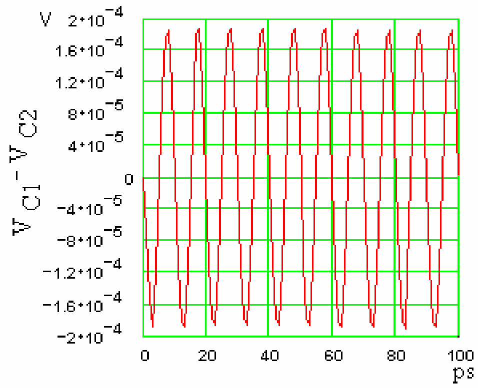


Fig.7 Twice output difference.



a) Outputs V_{C1} and V_{C2} versus time.



b) Output (V_{C1}-V_{C2}) as a function of time.

Fig.8 Simulation results for ac case.

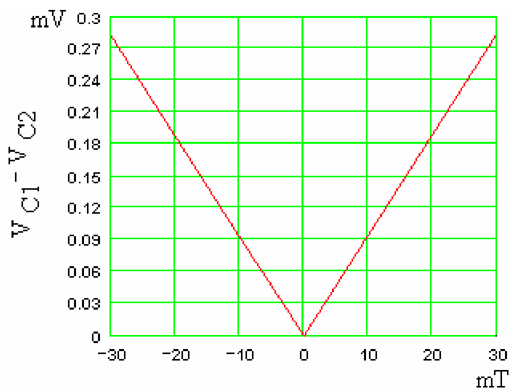


Fig.9 Output (V_{C1}-V_{C2}) against B.

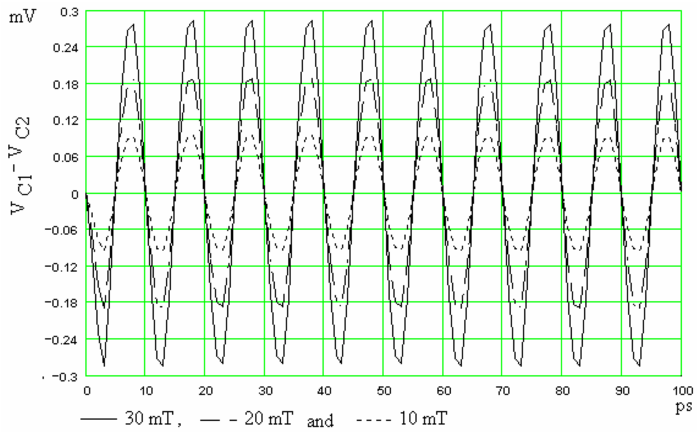


Fig.10 The effect of the magnitude of applyied field on the output voltage.

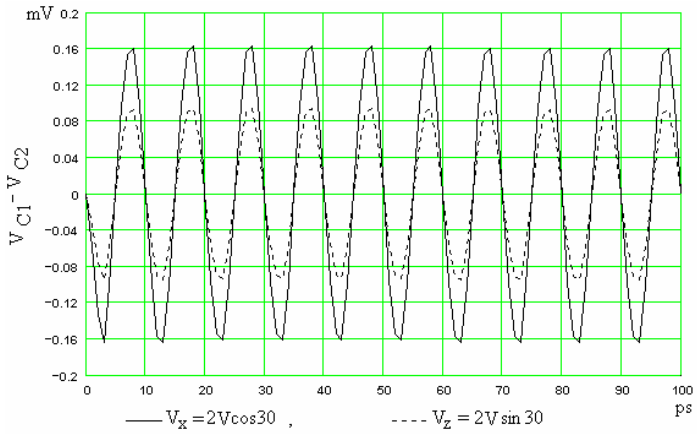


Fig.11 Field components x and z with 30 degree deflection from x-axis.

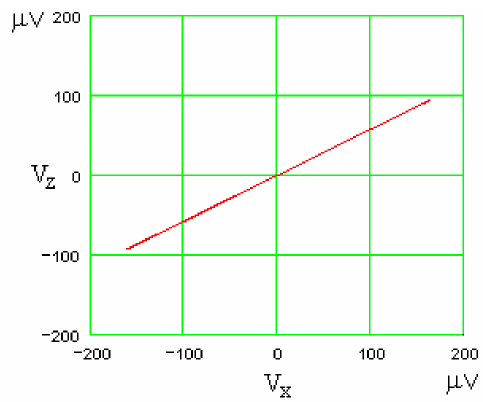


Fig.12 Orientation of the field vector makes 30 degree with x-axis.

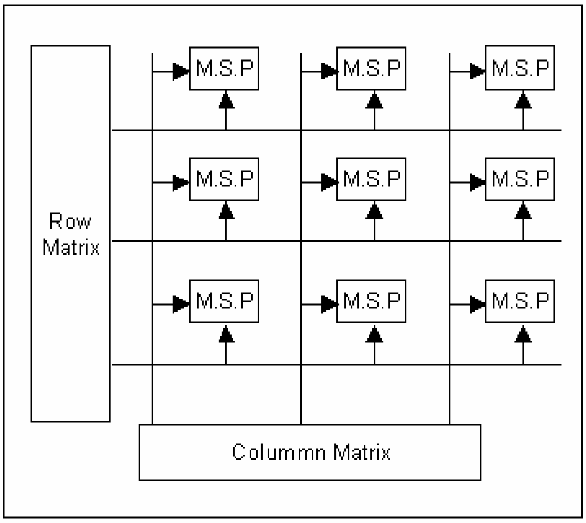


Fig.13 Linear Sensor Array Matrix.

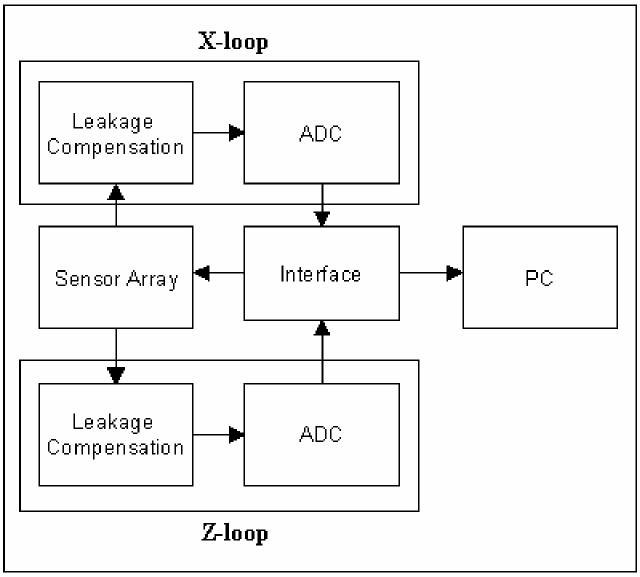


Fig.14 The proposed detection System.

REFERENCES

Andreas Witzig, R. Peter and F. Wolfgang. 1999. Global Modeling of Microwave Applications by Combining the FDTD Method and a General Semiconductor Device and Circuit Simulator. IEEE Trans. On Microwave Theory and Tech., pp. 919-928 .،

Alsunaidi,S. M.Sohel and S. El-Ghazaly.1996. Electromagnetic Wave Effects on Microwave Transistors Using a Full-Wave Time-Domain Model. IEEE Trans. On Microwave Theory and Tech., pp. 799-808 .،

El-Ghazaly. 1997. Electromagnetic Interfacing of Semiconductor Devices and Circuits. IEEE MTT-S Digest, pp. 151-154.،

Johannes, W. A. and A. Werner. 1999. An Analytical Model of MAGFET Sensitivity Including Secondary Effects Using a Continuous Description of the Geometric Correction Factor G. IEEE Trans. On Electron Devices, pp. 89-95.،

Nixon and A. Nathan. 1997. CCD-Based Magnetic Field Imaging. IEEE Trans. On Electron Devices, pp. 1653-1657.

Ramadan, A. El-Hennawy, Kamel Hassan, and Ali Abou Elnour.1999. Study and Characterization of a New MOSFET Voltage controlled Negative Resistance for Super Selective IC Tank Circuits. International Journal of Electronics, pp. 311-319.

Ramadan, El-Hennawy and Esam Yosry. 1996. Study and Characterization of a New MOSFET IC Reactance Device S-MOSFET Operated in the Exponential Mode. International Conference of Microelectronics (ICM), pp. 299-302, Dec .

Ristic, T. Smy and H. Baltes.1989. A Lateral Magneto Transistor Structure With a Linear Response to the Magnetic Field. IEEE Trans. On Electron Devices, pp. 1076-1086 .

Wiliam, and N. Arokia. 1993. Temperature Coefficient of Resolution of Lateral Bipolar Magnetotransistors. IEEE Trans. On Electron Devices, pp. 910-917.

APPENDIX

Notations

B	Magnetic induction's vector.
B_x	Magnetic field in x-direction.
B_z	Magnetic field in z-direction.
G	Geometrical correction factor .
G_x	Geometrical correction factor in x-direction.
G_y	Geometrical correction factor in y-direction.
I_{d0}	Total current collected by the collector at zero magnetic field.
I_d	Collector (drain) current.
I_{s0}	Total current collected by the substrate at zero magnetic field.
j_{nx}	Electron current density in x-direction.
j_{ny}	Electron current density in y-direction.
j_x	Current density in x-direction.
j_x^o	Current (in x-direction) before magnetic field.
j_z	Current density in z-direction.
J	Conduction current density.
J_n	Electron current density.
J_p	Hole current density.
K	Proportionality constant.
L_x	Lateral box length.
L_y	Vertical box length.
V	Output voltage.
V_x	Output voltage for x-direction.
V_z	Output voltage for z-direction .
W_x	Vertical box width.
W_y	Lateral box width.
δI	Current change due to magnetic field.
δI_d	Current change in the collector due to magnetic field.
δV	Voltage change due to magnetic field.
μ_H	Hall mobility.
μ_n	Electron mobility.
μ_p	Hole mobility.

Received 11/11/1424;03/01/2004, accepted 10 /02 /1425; 31/03/2004